Northwest Atlantic Fisheries Organization

Serial No. N5082 **NAFO SCR Doc. 05/7**

SCIENTIFIC COUNCIL MEETING – JUNE 2005

Environmental Conditions in the Labrador Sea in 2004

by

R. M. Hendry

Department of Fisheries and Oceans, Bedford Institute of Oceanography
PO Box 1006, Dartmouth, Canada B2Y 4A2
email: hendryr@mar.dfo-mpo.gc.ca

Abstract

The 15th annual occupation of the AR7W Labrador Sea section in May 2004 encountered warm and saline conditions at upper and intermediate levels, continuing a decade-long warming trend following several years of particularly cold conditions in the early 1990s. Changes in temperature and salinity averaged over the upper 150 m during this 15-year period amount to about 1°C and 0.1, respectively. The winter of 2003-2004 was particularly mild, giving the second lowest sea-air heat flux in the west-central Labrador Sea since 1987. Annual average 2004 sea surface temperature was more than 1°C warmer than normal in the west-central Labrador Sea. These changes reflect a northward shift of normal regional patterns of heat flux and sea surface temperature by several degrees of latitude.

Introduction and Summary

Labrador Sea hydrographic conditions depend on a balance between heat lost to the atmosphere and heat gained from warm and saline Atlantic Waters carried northward into the Labrador Sea by the West Greenland Current. Severe winters under high North Atlantic Oscillation (NAO) conditions lead to greater cooling: in exceptional cases, the resulting increases in the surface density can lead to convective mixing of the water column to depths of 2 km. Milder winters under low NAO conditions lead to lower heat losses and an increased presence of the warm and saline Atlantic Waters.

A sequence of severe winters in the early 1990s led to the most recent period of deep convection, which peaked in 1993-1994. Recent winters have been generally mild. Annual mean sea-air heat fluxes in the west-central Labrador Sea from the NCEP/NCAR Reanalysis project have been lower than normal since 1998. The 2004 annual mean of 39 W/m^2 was the second lowest since 1987. The January-March 2004 mean air-sea heat loss was the lowest since 1987 and the sixth lowest in the 1948-2004 NCEP Reanalysis time period.

Mean 2004 sea surface temperatures in the west-central Labrador Sea from the UK Met Office Hadley Centre HadISST 1.1 Global Sea Surface Temperature data set were the warmest in the past 45 years.

Sea level in the west-central Labrador Sea was about 6 cm higher in 2004 than during the early 1990s, based on TOPEX/POSEIDON and JASON-1 altimetry. Most of this change can be related to changes in hydrographic conditions. There has been relatively little change in annual-mean sea level in the west-central Labrador Sea during the past few years.

Ocean Sciences Division, DFO Maritimes Region has monitored hydrographic properties on the AR7W line across the Labrador Sea in the early summer of each year since 1990. The 15th annual AR7W survey took place in late May

2004. Between 1990 and 2004 there has been a general trend to warmer and saltier conditions in the upper layers of the Labrador Sea. Changes in temperature and salinity averaged over the upper 150 m during this period amount to about 1°C and 0.1 respectively.

Below the seasonal layer, the upper waters (averages over 150-1 000 m or 150-1 500 m) of the west-central Labrador Sea have become steadily warmer and more saline over the past four years. By this measure, conditions in 2004 were the warmest and saltiest in the 15 years of annual AR7W surveys. Density changes during the past few years have been relatively small, with changes linked to temperature and salinity nearly in balance.

The May 2004 survey encountered warm and saline conditions in waters in the offshore branch of the West Greenland Current, with maximum salinities greater than 34.95. High salinity near-surface waters extended westward into the central Labrador Sea.

The May 2004 observations suggest that the 2003-2004 winter mixed layer had maximum potential density anomalies just less than 27.73 kg/m^3 and maximum depths of about 800 m, less than the corresponding values attained following the winter of 2002-2003 as observed in the 2003 AR7W survey.

Results and Discussion

General Environmental Indicators

Sea-air heat flux

On an annual average, the Labrador Sea loses heat to the overlying atmosphere. The greatest heat losses occur in January and February. Monthly-averaged air-sea flux fields are available from the co-operative Reanalysis Project (Kistler *et al*., 2001) of the U.S. National Centers for Environmental Prediction (NCEP) and National Center for Atmospheric Research (NCAR).

Figure 1(a) shows a map of 2004 mean NCEP Reanalysis sea-air heat flux for the Labrador Sea. Positions of the NCEP grid points are superimposed on the map. AR7W station positions occupied in May 2004 on CCGS Hudson Mission 2004-016 and the position of former Ocean Weather Station (OWS) Bravo are also marked on the map. The four highlighted stations near the OWS Bravo site are used to represent conditions in the west-central Labrador Sea. Figure 1(b) shows a similar map of 1971-2000 mean sea-air heat flux. The 30-year period 1971-2000 is used to represent normal conditions. The patterns are similar, but the maximum in the heat loss pattern for 2004 is displaced about 100 km to the northwest compared to the normal pattern. Figure 1(c) shows a map of the 2004 anomaly in sea-air heat flux relative to normal conditions. Values in the west-central Labrador Sea in 2004 were 20-30 W/m^2 less than normal. Figure 1(d) shows a time series of interannual changes in annual mean and annual mean plus residual seasonal variability in sea-air heat flux from the NCEP Reanalysis grid point at 56.2N, 52.5W. The normal value is 66 W/m^2. The seasons are defined as January-March (JFM), April-June (AMJ), July-September (JAS), and October-December (OND). The residual seasonal variability is the residual after a normal seasonal cycle is removed. The normal seasonal cycle was defined by a least-squares fit of annual plus semiannual harmonics to monthly mean heat fluxes for 1971-2000. Annual mean heat losses at this location have been less than normal for the past seven years. The 2004 annual mean of 39 W/m^2 was the second lowest since 1987, with 2001 being the lowest. The JFM 2004 seasonal residual was the lowest since 1987 and the sixth lowest in the 1948-2004 NCEP Reanalysis time period.

Sea-surface temperature

The UK Met Office Hadley Centre produces HadISST 1.1, global estimates of monthly mean sea-surface temperature (SST) on a one degree by one degree latitude-longitude grid. Figure 2(a) shows a map of 2004 mean SST from this source for the Labrador Sea annotated with AR7W and OWS Bravo positions as in Fig. 1(a). Figure 2(b) shows a similar map of 1971-2000 mean SST. The 2004 map and the normal map show similar patterns, but again the isotherms in the 2004 map are displaced about 100 km to the northwest compared to the normal pattern. Figure 1(c) shows a map of the 2004 SST anomaly relative to normal conditions. Values in the west-central Labrador Sea in 2004 were more than 1°C warmer than normal. Figure 1(d) shows a time series of annual mean and annual mean plus residual seasonal variability averaged over nine grid points centred at 56.5N, 52.5W. The normal value is 4.34°C. The residual seasonal variability is the residual after removal of a normal seasonal cycle defined in

the same way as discussed above for heat flux. Annual mean SST at this location has been warmer than normal since the mid-1990s. Both the 2004 annual mean and the 2004 JFM seasonal residual were record highs for 1960-2004.

Sea level

The French SSALTO/DUACS group uses TOPEX/POSEIDON and JASON-1 altimetric sea level measurements to produce weekly gridded Maps of Sea Level Anomalies (MSLA) with near-global geographic coverage on a 1/3° Mercator grid. These are distributed by the French AVISO group with support from the French national space agency CNES. Data coverage begins with the TOPEX/POSEIDON mission in late 1992 and continues to the present.

Figure 3(a) shows a map of 2004 mean sea level anomaly (SLA) from this source for the Labrador Sea annotated with AR7W and OWS Bravo positions as Figure 1(a). The ground tracks common to the two altimetric missions involved are also shown. The gridded MSLA are produced by a statistical interpolation that is most reliable at points close to the measurements (Le Traon, *et al.*, 1998). The anomalies are shown relative to the mean value for 1993-2004. The map shows positive SLA values in the west-central Labrador Sea in 2004 ranging from 2 to 4 cm. There is a local minimum with values below 2 cm at the ground track crossover point near the highlighted AR7W stations used to represent the west-central Labrador Sea. Figure 3(b) shows a time series of annual mean and residual seasonal SLA from an average over 25 grid points centred at 56.7N, 52.3W near this crossover point. The normal seasonal cycle was defined by a least-squares fit of annual plus semiannual harmonics to weekly values of SLA for 1993-2004. Sea level showed a marked rise at this location from the mid-1990s to 2000, and has been relatively constant since then. The 2004 annual mean value is slightly less than the annual mean 2003 value. These values are somewhat sensitive to the spatial averaging. A larger spatial average includes 2004 SLA grid points with anomalies greater than 4 cm and gives 2004 values slightly higher than 2003. The 2003 annual mean SLA field (not shown) was less spatially variability in the west-central Labrador Sea than 2004.

AR7W hydrography

Figure 4 shows a map of the Labrador Sea with AR7W station positions occupied in May 2004 on CCGS Hudson Mission 2004-016 under the scientific direction of Dr. Glen Harrison. The 28 principal AR7W stations were occupied during the period May 20-26, 2004. The standard section spans approximately 880 km from the 130 m contour on the inshore Labrador shelf to the 200 m contour on the West Greenland shelf. Sea ice sometimes limits coverage at the ends of the section. Only the two stations nearest the Labrador coast were unreachable in 2004 even though it was relatively early in the season.

Contoured gridded sections of potential temperature and salinity as observed in May 2004 are shown in Fig. 5(a) and 5(b). Along-section distance in kilometres increasing from southwest (Labrador) to northeast (Greenland) is used as the horizontal coordinate. The four stations chosen to represent conditions in the west-central Labrador Sea lie within the 320-520 km distance range.

Notable in the upper levels of Fig. 5(a) (potential temperature) are cold waters ($<2^{o}$C) over the Labrador Shelf. Similarly cold waters in the upper few hundred metres over the outer edge of the West Greenland shelf are associated with the inshore branch of the northward-flowing West Greenland Current. Warmer waters ($>4^{o}$C) in the upper 500 m of the water column over the West Greenland slope are associated with the offshore branch of the West Greenland Current.

There is a regular seasonal cycle in both temperature and salinity that affects the uppermost layers. Near-surface seasonal warming and freshening is apparent in Fig. 5(a) and 5(b), respectively.

Several extra stations were made to better define a mesoscale eddy which shows up prominently in the potential temperature and salinity fields near the 650 km mark.

In the central Labrador Sea, water at depths between 600 m and 1 200 m below the seasonal thermocline has reduced vertical temperature gradients that mark vertically-mixed Labrador Sea Water (LSW) formed by winter convection in recent years. The LSW layer creates a relative minimum in potential temperature with core values near 3.2°C. The section plots are annotated with the pressure of this relative minimum in potential temperature. The

LSW layer extends over much of the section, but it is most prominent in the west-central Labrador Sea where the deepest winter mixed layers are formed. Waters in the upper 500 m on the Greenland side are notably warmer than on the Labrador side, showing a greater influence of the warm Irminger Waters. Denser components of the warm and saline Irminger Water influence a layer centred near 1 500 m below the LSW. The intrusion of these warm and saline waters creates a relative maximum in potential temperature with maximum values greater than 3.3°C. The section plots also show the pressure of this intermediate-depth potential temperature maximum.

In the salinity section in Fig. 5(b), waters in the upper 500 m on the Greenland end of the section are notably saltier than waters in the same depth range on the Labrador end, again showing the Irminger Water influence. Traces of relatively fresh water with salinity less than 34.88 near 2 000 m depth are remnants of the deep convection of the early 1990s.

Changes in upper level properties

The strongest seasonal variations occur in the upper 150 m of the water column. Survey times during the 15-year period varied from late May to late July. Climatological hydrographic data from the U.S. National Ocean Data Center (Conkright *et al*., 2002) were used to estimate seasonal changes in potential temperature and salinity averaged over 0-150 m depths in the west-central Labrador Sea. The inferred seasonal effects were then removed from the AR7W survey data. Figures 6(a) and 6(b) show time series of 0-150 m deseasoned mean potential temperature and salinity for stations in the 320-520 km distance range for the 15 spring and early summer AR7W occupations from 1990 to 2004. For example, the 2004 value is an average over the four highlighted stations in Fig. 4. Standard deviations of individual 0-150 m station means for each survey are indicated on the plots. The 15-year changes in potential temperature and salinity estimated by least-squares regressions are about 1.1°C and 0.09, respectively. Anomalies for 2004 relative to the1990-2004 mean are 0.4°C in potential temperature and 0.03 in salinity. The 2003 potential temperature anomaly from late July 2003 was still greater. The summer of 2003 in the Labrador Sea was evidently a particularly warm one. The same feature is seen in sea surface temperature. The HadISST 1.1 2003 JAS residual in the west-central Labrador Sea was the highest in the 1960-2004 analysis period.

Water masses

As an overview of the water masses in the Labrador Sea, Fig. 7(a) shows a potential temperature – salinity scatter diagram for all 2004 AR7W stations. Four water types are singled out for attention:

- Irminger Atlantic Water (IAW) with potential temperatures between 4°C and 6°C and salinities between 34.95 and 35.10 (Lee, 1968);
- Irminger Mode Water (IMW) with potential temperatures between 4°C and 6°C and salinities between 34.85 and 34.95 (Buch, 2000);
- Labrador Current Water (LCW) with potential temperatures between -1.8°C and 1°C and salinities between 32 and 34; and
- Labrador Sea Water (LSW) with potential temperatures between 3.2°C and 3.3°C and salinities between 34.82 and 34.88.

The last two definitions are nominal ones, for illustration only. LSW produced during the early 1990s had potential temperature near 2.8°C.

Figures 7(b) – 7(d) show contoured gridded sections of potential density anomaly, potential vorticity, and apparent oxygen utilization (AOU), respectively.

In principle, mixed layers formed by overturning surface waters will have initial values of zero for both potential vorticity and AOU. To the extent that these properties are conserved, they can be used to trace waters that originated in the winter mixed layers of the Labrador Sea.

Pressure ranges on stations where IAW and IMW potential temperature - salinity water types as defined above were found are highlighted in the section plots with the same colour scheme used in Fig. 6(a). The IAW and IMW types are confined to the upper levels on the West Greenland end of the AR7W section. They are associated with

relatively low values of potential density and relatively high values potential vorticity. IMW has been observed on the AR7W surveys in recent years. Higher salinity waters meeting the Lee (1968) IAW criterion were also seen in the 2003 survey and in a December 2002 survey, but not in 2001 or 2002.

The eddy centred near 650 km shows up prominently in all three fields.

Regions of relatively low apparent oxygen utilization near 2 000 m correspond to relatively high dissolved oxygen. They are further remnants of the deep convection of the early 1990s.

Interannual changes in winter convection

Figure 8 provides an overview of interannual variability from AR7W surveys since 1990. It shows a time series of the pressure on selected potential density anomaly surfaces from average profiles in the 320-520 km distance range for each survey as a function of the median station time. This provides an update of Fig. 4 in Lazier *et al.* (2002).

The deep convection of the early 1990s is reflected in the 1993-1995 maximum in the separation of the 27.77 and 27.79 kg/m^3 potential density anomaly surfaces bounding the deeper shaded layer in Fig. 8. The volume of water in this potential density range decreased steadily from 1995 to 2000. Pressures corresponding to the minimum potential temperature in the 27.77-27.79 kg/m^3 layer for each survey are noted in the figure. The prominent relative minimum in potential temperature in this layer created by the deep convection in the winters of 1992-1993 and 1993-1994 persists until at least 1999. Changes in the separation of these isopycnals have been small since 2000.

Since 1999 or 2000 and especially from 2001 to 2003 there has been an increase in the separation of isopycnals with potential density anomalies in the range 27.72-27.75 kg/m^3 that define the shallower shaded layer in Fig. 8. In 2000, this layer developed a prominent relative minimum in potential temperature with core potential temperature 3.2°C, salinity 34.83, and potential density anomaly 27.73 kg/m^3. A relative minimum in potential temperature is also present in 2002 and 2003 at increasing values of potential density anomaly. This persistent feature can be interpreted as a remnant of intermediate-depth winter convection in the west-central Labrador Sea during recent years. In 2004 the minimum potential temperature in the 27.72-27.75 kg/m^3 layer is found near the bottom of the layer.

Figures 9(a)-9(b) show average profiles of potential temperature and low-pass filtered potential vorticity for stations in the 320-520 km distance range from the 2000-2004 spring and early summer AR7W occupations. Potential vorticity has been smoothed in the vertical to emphasize vertical scales of 200 m and greater. The properties are averaged on potential density surfaces and plotted against potential density anomaly. The four individual stations included in the 2004 average are shown in the background for each of the figures.

Figure 9(a) shows the relative minima in potential temperature introduced in Fig. 8 at progressively higher potential densities: from 27.73 kg/m^3 in 2000 and 2001, to greater than 27.73 kg/m^3 for 2002 and 2003, to greater than 27.74 kg/m^3 in 2004. The potential temperature at the 2004 relative minimum is about 0.07°C warmer than for the previous two years. Figure 9(b) shows similar relative minima in potential vorticity at about the same potential density anomalies. Waters with potential density anomalies less than 27.72 kg/m^3 are replaced annually, so their properties vary seasonally. The 2000, 2001, and 2004 surveys took place in late May or early June. The 2002 and 2003 surveys took place in early and late July, respectively.

It is not immediately obvious if the relative minima in potential temperature and potential vorticity observed in 2004 are remnants of convection during the winter of 2003-2004 or remnants of convection during a previous winter. In the latter case, mixing would tend to increase the values of potential temperature and potential vorticity at the respective relative minima.

Figure 9(c) shows similar profiles of potential vorticity and apparent oxygen utilization (AOU) averaged on pressure surfaces and plotted as a function of pressure. Figure 9(c) is identical to Fig. 9(b) with pressure substituted for potential density anomaly as the independent variable. The 27.72-27.74 kg/m^3 layer in Fig. 9(a) corresponds to pressures from 360 to 1 250 dbar in Fig. 9(c).

Figure 9(d) shows larger differences in the vertical structure in AOU for 2002-2004 than seen in potential vorticity (calibrated CTD oxygen data for 2000 and 2001 were not available for this report). In particular, 2003 shows a layer

from 700-1 200 dbar with nearly constant AOU near 0.6 mL/L. This pressure range corresponds to the low potential vorticity layer in Fig. 9(c). It includes potential density anomalies in the range 27.73-27.74 kg/m^3. The 2004 survey shows a generally strong increase in AOU with increasing pressure in the same pressure range. The exception is the 700-800 dbar range in which AOU is also nearly constant with about the same 0.6 mL/L value. The potential density anomaly is just less than 27.73 kg/m^3 in this range of pressures. The appreciable gradients in AOU deeper than about 800 dbar suggest that the convective mixed layer formed in the winter of 2003-2004 did not reach potential density anomalies greater than 27.73 kg/m^3, corresponding to a maximum depth of about 800 m.

Interannual changes in heat, salt, buoyancy, and geopotential

The changes in heat and salt from 1990 to 2000 were discussed by Lazier *et al*. (2002). Time series of the changes in heat, salt, buoyancy, and geopotential in selected layers from spring and early summer AR7W surveys from 1990 to 2004 are shown in Fig. 10(a)-10(d). Each series is plotted as an anomaly relative to its 1994 value. Any averages involving the 0-150 dbar range have been corrected for seasonal changes in the 0-150 dbar layer as discussed above.

The ranges of heat and salt content in the 0-2 000 dbar layer in Fig. 10(a) and 10(b) are approximately 5 GJ/m^2 and 100 kg,respectively. A heat gain of 1 GJ/m^2 by this layer would increase its mean temperature by about 0.12°C. An increase of 20 kg/m^2 of salt in the same layer raises its mean salinity by about 0.01.

The heat content in the 0-1 500 and 0-2 000 dbar layers increased in 2004 compared to 2003. This continued a 4-year increasing trend and gave 2004 the highest values observed in the 15 spring and early summer AR7W surveys. The heat content of the 0-1 000 dbar layer in 2004 was nearly identical to the 2003 value because the 0-150 dbar layer was warmer in 2003.

The salt content of the 0-1 000 dbar layer shows more-random changes than the heat content. Since 2001, however, the salt content of this layer shows an increasing trend. The 2004 value is the highest in the record. The 1 000-1 500 dbar and 1 500-2 000 dbar layers show much smoother changes in salt content with time. The salt content in both deep layers increased steadily from 1994 to 2000 or 2001, when the shallower recent convection regime began to establish itself. Salt content decreased in the 1 000-1 500 dbar layer between 2001 and 2003. This is related to the deepening of isopycnal surfaces in that pressure range and an increased presence of lower density and lower salinity water in the 1 000-1 500 dbar pressure range. In contrast, the 1 500-2 000 dbar layer shows a steady increase in salt content since 1994. The net result is that the salt content, or equivalently the mean salinity, in the 0-2 000 dbar range has increased for each of the past four years. The 2004 value is a record high.

Higher temperatures correspond to lower water densities and higher salinities correspond to greater water densities. The trends to warmer and saltier conditions have opposite effects on density or buoyancy. Fig. 10(c) shows changes in buoyancy relative to 1994 associated with the same pressure layers as dealt with in Fig. 10(a)-10(b). The warming of the upper 1 000 dbar layer from 1994 to 1999-2000 while salinity remained relatively constant produced a large increase in buoyancy. Recent years have seen both warmer and saltier upper-layer conditions. There is no clear trend in buoyancy over the past six years.

Figure 10(d) shows time series of the changes in geopotential at the minimum layer pressure relative to the maximum layer pressure for four of the same layers featured in Fig. 10(c). The geopotential changes are all relative to 1994 values. Also shown are time series of annual mean and annual mean plus seasonal residual sea surface geopotential relative to the 1994 annual mean derived from the satellite altimetry. These correspond to the sea level anomaly time series in Fig. 3(b). There is close agreement between the 0-2 000 dbar geopotential difference from hydrography and geopotential changes related to changing sea level. Another way of putting this is that the sea level changes are largely explained by steric effects in the upper 2 000 m of the water column. Hydrographic changes in the upper 1 000 m have the greatest effect in sea level, but changes deeper than 1 000 m also have an appreciable influence.

Acknowledgments

Dr. R. Allyn Clarke at the Bedford Institute of Oceanography has provided overall scientific direction to the AR7W repeat hydrography programme for many years. Dr. Glen Harrison at the Bedford Institute of Oceanography was Chief Scientist of CCGS Hudson Mission 2004-016 for the most-recent AR7W occupation.

The HadISST 1.1 Global Sea Surface Temperature data set was provided by the Hadley Centre for Climate Prediction and Research, Met Office, Bracknell, UK. [http://www.metoffice.com/research/hadleycentre/obsdata/HadISST1.html]

Data from the NCEP Reanalysis were provided by the NOAA-CIRES Climate Diagnostics Center, Boulder, Colorado, USA, from their Web site at http://www.cdc.noaa.gov/.

MSLA altimeter products were provided by the French AVISO/Altimetry operations centre at the CLS Space Oceanography Division. [http://www.aviso.oceanobs.com/]

Climatological hydrographic data were provided by the U.S. National Oceanographic Data Center. [http://www.nodc.noaa.gov/].

References

BUCH, E. 2000. Air-sea-ice conditions off southwest Greenland, 1981-97. *Journal of Northwest Atlantic Fishery Science*, **26**: 123-126.

CONKRIGHT, M.E., R. A. Locarnini, H.E. Garcia, T.D. Brien, T.P. Boyer, C. Stephens,

ANTONOV, J. I. 2002. World Ocean Atlas 2001. National Oceanographic Data Center Internal Report 17, 17 pp.

KISTLER, R., E. KALNAY, W. COLLINS, S. SAHA, G. WHITE, J. WOOLLEN, M. CHELLIAH, W. EBISUZAKI, M. KANAMITSU, V. KOUSKY, H. VAN DEN DOOL, R. JENNE, and M. FIORINO. 2001. The NCEP-NCAR 50-Year Reanalysis. Bulletin of the American Meteorological Society, **82**: 247-268.

LAZIER, J., R. HENDRY, A. CLARKE, I. YASHAYAEV, and P. RHINES. 2002. Convection and restratification in the Labrador Sea, 1990-2000. Deep Sea Research, **49**: 1819-1835.

LEE, A. 1968. NORWESTLANT Surveys: Physical Oceanography. ICNAF Special Publication 7(I): 31-54.

LE TRAON, P.-Y., F. NADAL, and N. DUCET.1998. An improved mapping method of multisatellite altimeter data. Journal of Atmospheric and Oceanic Technology, **15**, 522-534.

RAYNER, N. A., D. E. PARKER, E. B. HORTON, C. K. FOLLAND, L. V. ALEXANDER, D. P. ROWELL, E. C. KENT, and A. KAPLAN. 2003. Global analyses of sea surface temperature, sea ice, and night marine air temperature since the late nineteenth century. Journal of Geophysical Research, 108(D14), 4407, doi:10.1029/2002JD002670.

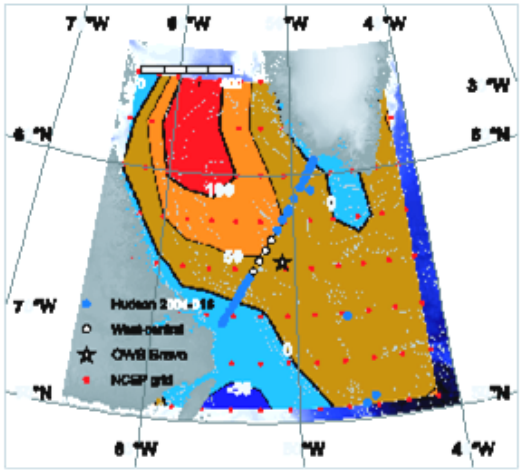

Fig. 1(a) NCEP/NCAR Reanalysis 1 mean sea-air heat flux (W/m^2) over the Labrador Sea for 2004 from monthly mean flux fields on a T62 Gaussian grid.

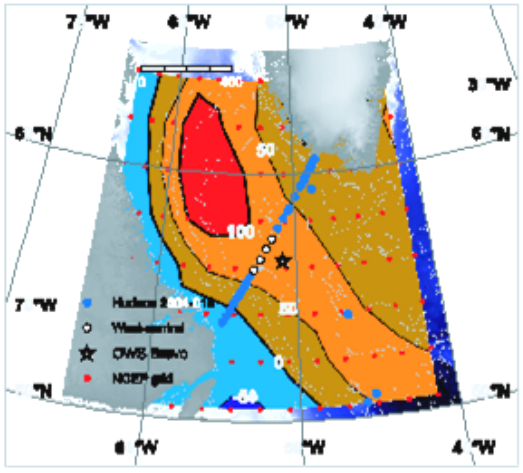

Fig. 1(b) NCEP/NCAR Reanalysis 1 annual mean sea-air heat flux (W/m^2) over the Labrador Sea for the 30-year normal period 1971-2000.

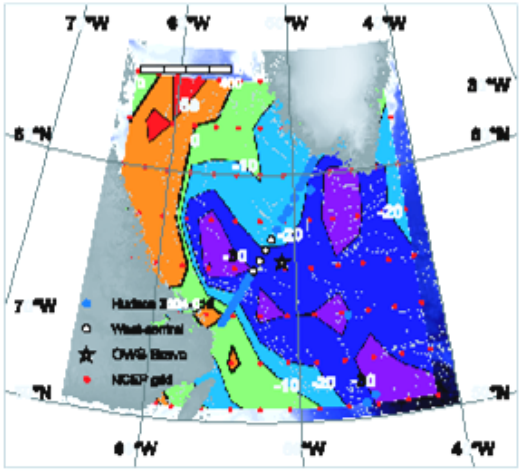

Fig. 1(c) Sea-air heat flux anomaly (W/m^2) over the Labrador Sea for 2004 relative to 1971-2000.

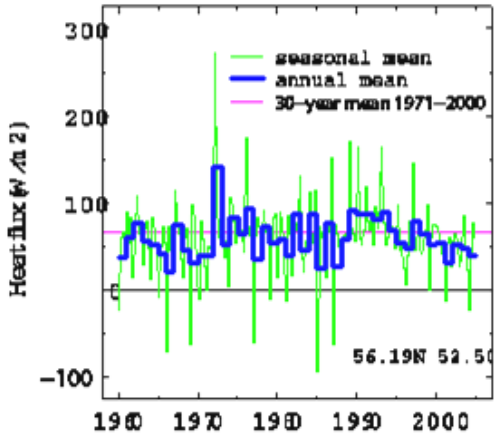

Fig. 1(d) Time series of annual mean and annual mean plus seasonal residual NCEP/NCAR Reanalysis 1 sea-air heat flux from 56.2N, 52.5W in the west-central Labrador Sea. The normal value is 66 W/m^2.

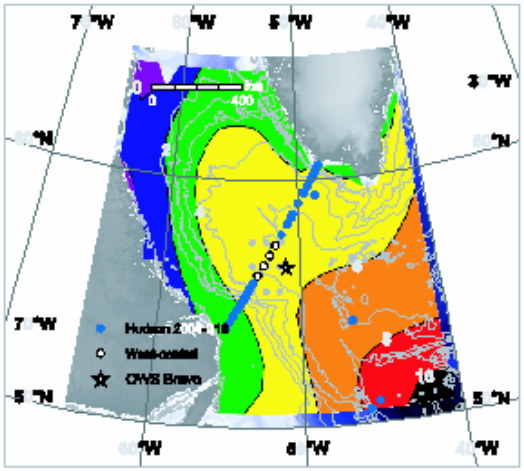

Fig. 2(a) HadISST 1.1 mean sea surface temperature (°C) over the Labrador Sea for 2004 from monthly mean values on a 1 degree x 1 degree grid.

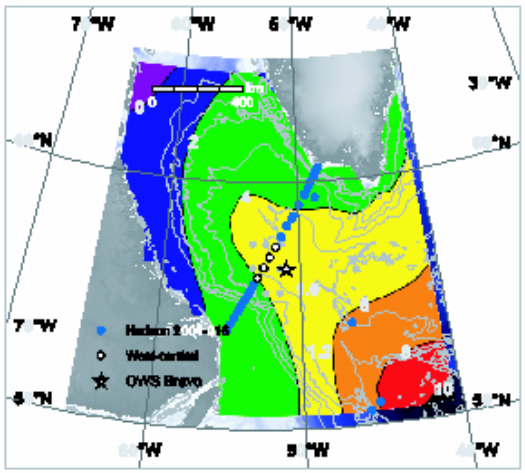

Fig. 2(b) HadISST 1.1 mean sea surface temperature (°C) over the Labrador Sea for the 30-year normal period 1971-2000.

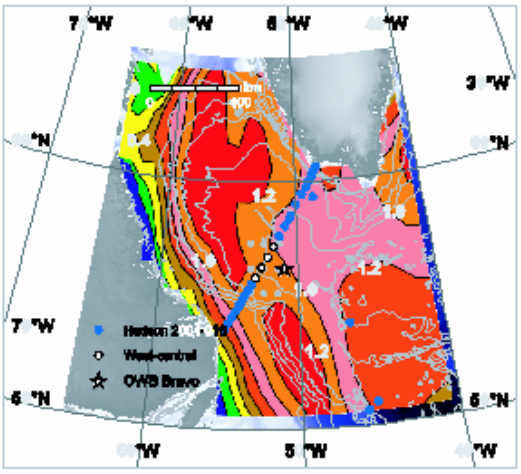

Fig. 2(c) HadISST 1.1 SST anomaly (°C) over the Labrador Sea for 2004 relative to 1971-2000.

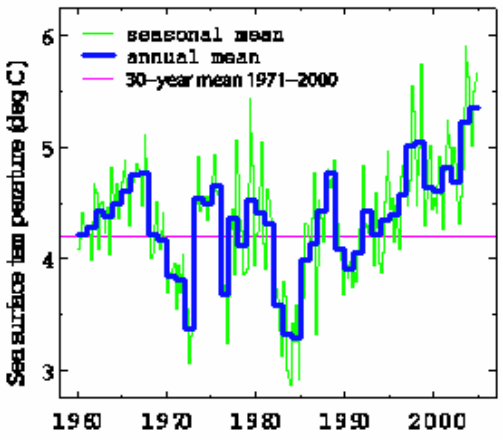

Fig. 2(d) Time series of annual mean and annual mean plus seasonal residual HADISST 1.1 SST averaged over 9 grid points centred at 56.5N, 52.5W in the west-central Labrador Sea. The normal value is 4.34°C.

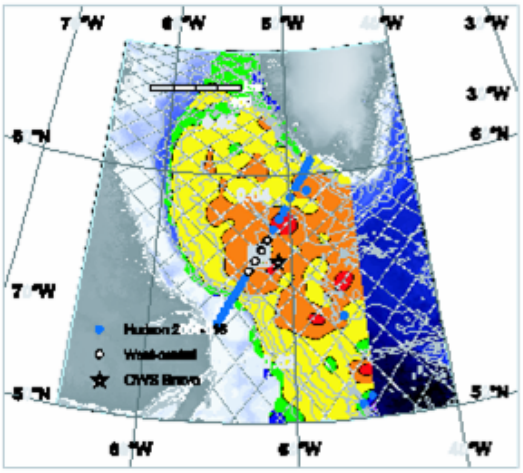

Fig. 3(a) Aviso mean SLA (m) for 2004 relative to 1993-2004 over the Labrador Sea from anomalies at 7-day intervals on a 1/3 degree Mercator grid. Topex/Poseidon – Jason-1 ground tracks are also shown.

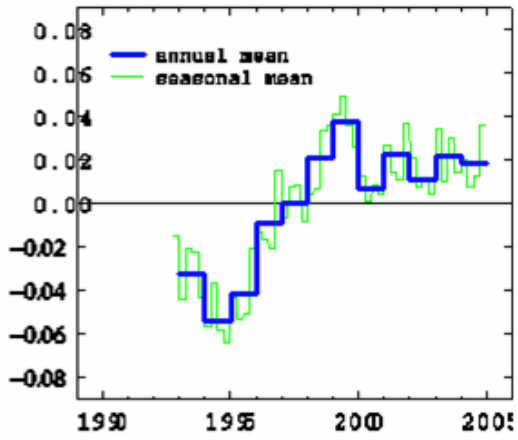

Fig. 3(b) Time series of annual mean and annual mean plus seasonal residual Aviso SLA relative to 1993-2004 averaged over 25 grid points centred at 56.7N, 52.5W in the west-central Labrador Sea.

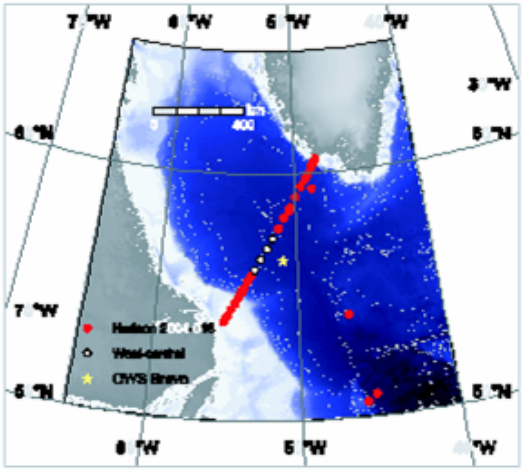

Fig. 4 Map of the Labrador Sea showing station positions from CCGS Hudson Mission 2004-016 during May 15-30, 2004 including the 2004 occupation of AR7W. The highlighted stations are used to represent conditions in the west-central Labrador Sea in subsequent figures.

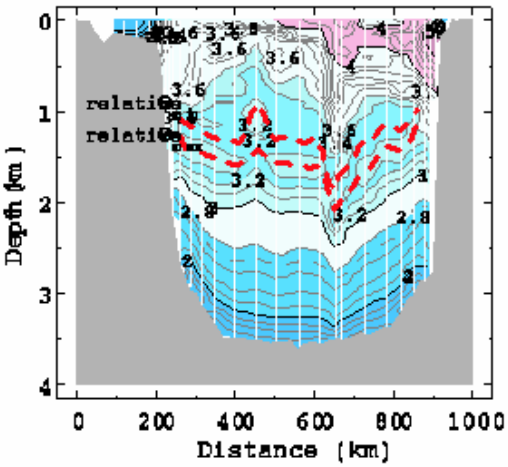

Fig. 5(a) Potential temperature (°C) on the AR7W section in late May 2004. Station positions are indicated by vertical lines. The dashed lines trace layers of relative minimum and maximum potential temperature.

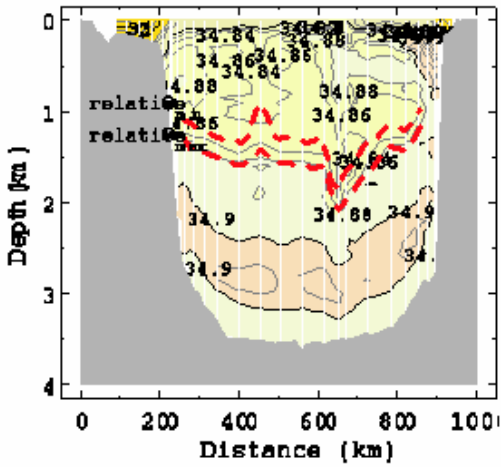

Fig. 5(b) Salinity on the AR7W section in May 2004 as in Fig. 5(a).

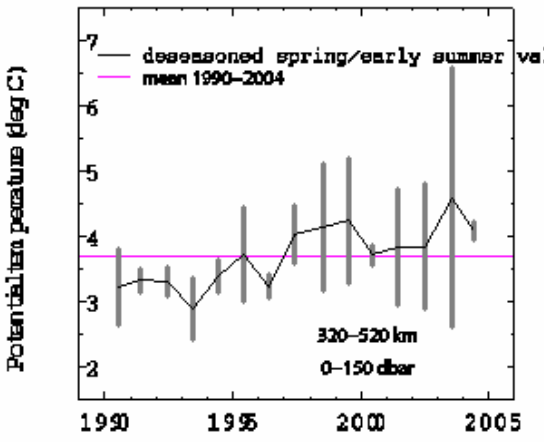

Fig. 6(a) Mean 0-150 m deseasoned potential temperature averaged over stations in the 320-520 km distance range for spring and early summer AR7W occupations. Error bars are among-station standard deviations of 0-150 m means for each cruise.

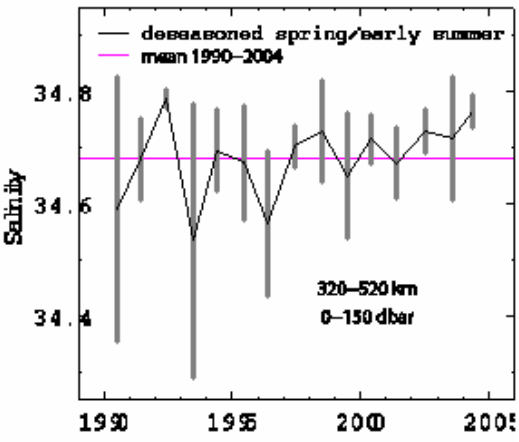

Fig. 6(b) Mean 0-150 m deseasoned salinity averaged over stations in the 320-520 km distance range for spring and early summer AR7W occupations as in Fig. 6(a).

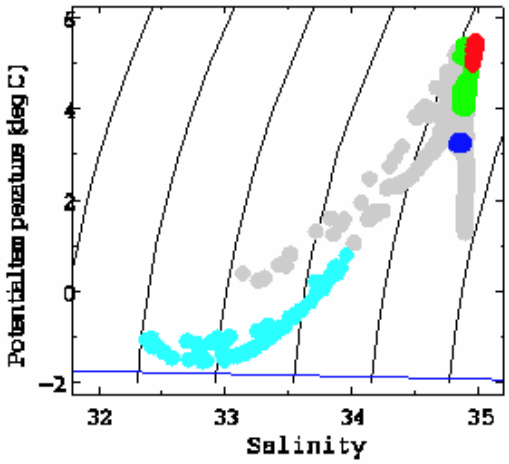

Fig. 7(a) Potential temperature – salinity scatter diagram from the May 2004 AR7W section. Highlighted water types LC (cyan), LSW (blue), IAW (red), and IMW (green) are defined in the text.

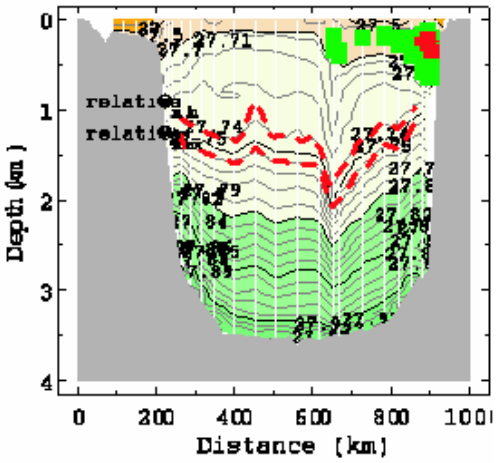

Fig. 7(b) Potential density anomaly (kg/m^3) on the AR7W section in late May 2004 as in Fig. 5(a). Water types IAW (red) and IMW (green) are highlighted as in Fig. 7(a).

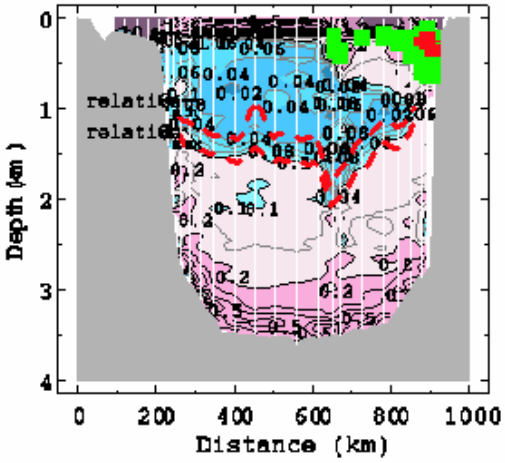

Fig. 7(c) Potential vorticity [10^{-10} (m·s)$^{-1}$] on the AR7W section in late May 2004 as in Fig. 5(a). Water types IAW (red) and IMW (green) are highlighted as in Fig. 7(a).

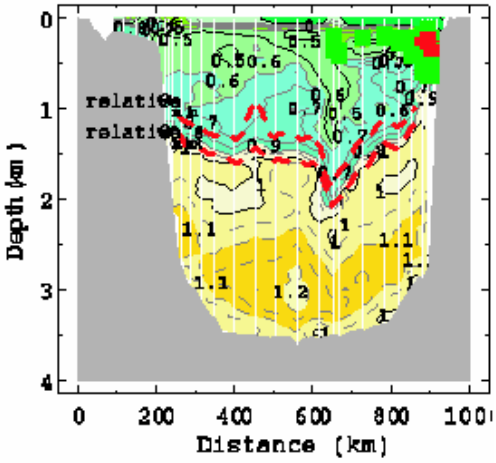

Fig. 7(d) Apparent oxygen utilization (mL/L) on the AR7W section in late May 2004 as in Fig. 5(a). Water types IAW (red) and IMW (green) are highlighted as in Fig. 7(a).

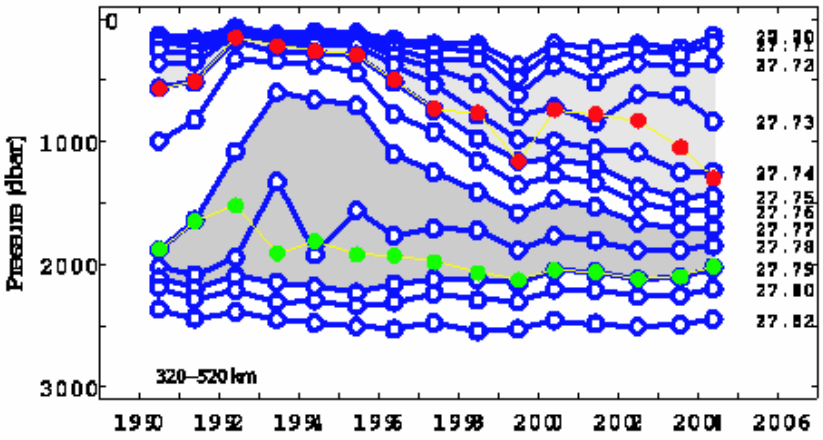

Fig. 8 Time series of pressure on selected potential density surfaces as labelled averaged over stations in the 320-520 km distance range on AR7W spring and early summer occupations during 1990-2004. Filled symbols mark pressures at minima in potential temperature in two shaded layers 27.72–27.75 kg/m^3 (upper) and 27.77–27.79 kg/m^3 (lower). The density surfaces in the lower layer were exposed to the atmosphere in winters in the early 1990s. A shallower winter convection regime appears to have been established beginning in 2000.

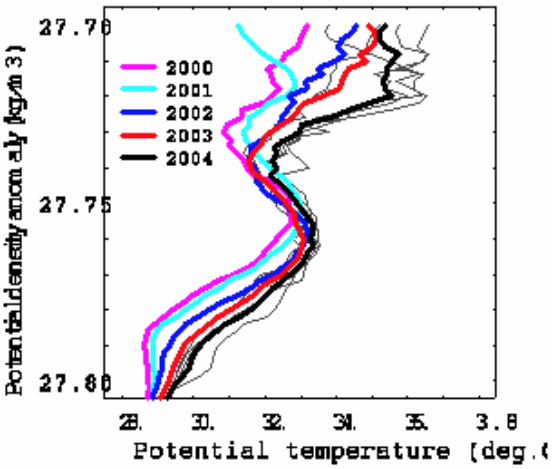

Fig. 9(a) Average potential temperature for stations in the 320-520 km distance range plotted against potential density anomaly for 2000-2004 spring and early summer AR7W occupations. Individual 2004 stations are shown in the background.

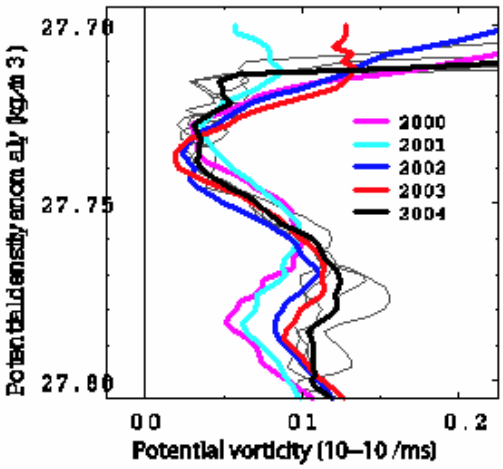

Fig. 9(b) Low-pass filtered potential vorticity averaged on potential density surfaces for stations in the 320-520 km distance range plotted against potential density anomaly for 2000-2004 spring and early summer AR7W occupations as in Fig. 9(a).

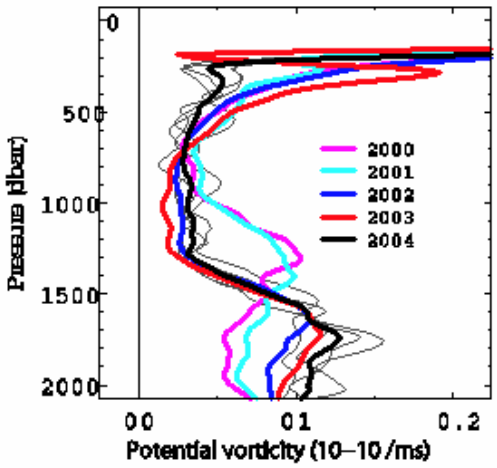

Fig. 9(c) Low-pass filtered potential vorticity averaged on pressure surfaces for stations in the 320-520 km distance range plotted against pressure for 2000-2004 spring and early summer AR7W occupations as in Fig. 9(a).

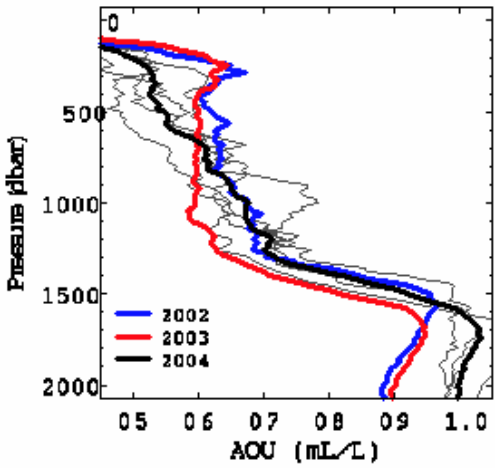

Fig. 9(d) Apparent oxygen utilization (AOU) averaged on pressure surfaces for stations in the 320-520 km distance range plotted against pressure for 2002, 2003, and 2004 spring and early summer AR7W occupations as in Fig. 9(a).

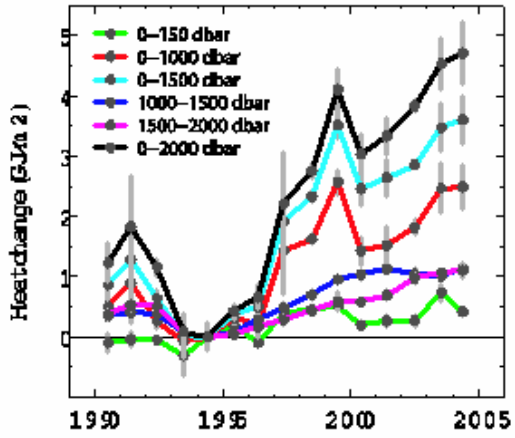

Fig. 10(b) Heat content in selected layers relative to the 1994 value from spring and early summer AR7W occupations averaged over stations in the 320-520 km distance range. Estimated 0-150 dbar seasonal changes have been remove.

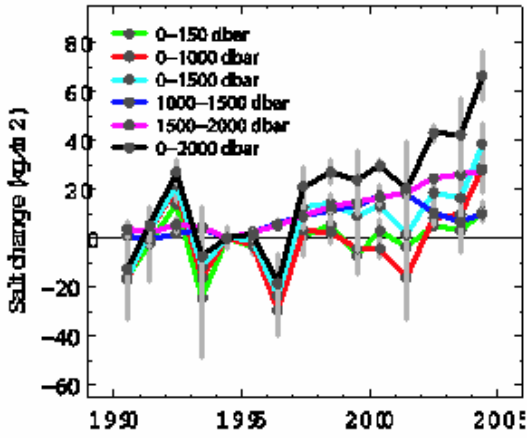

Fig. 10(h) Salt content in selected layers relative to the 1994 value from spring and early summer AR7W occupations averaged over stations in the 320-520 km distance range as in Fig. 10(a).

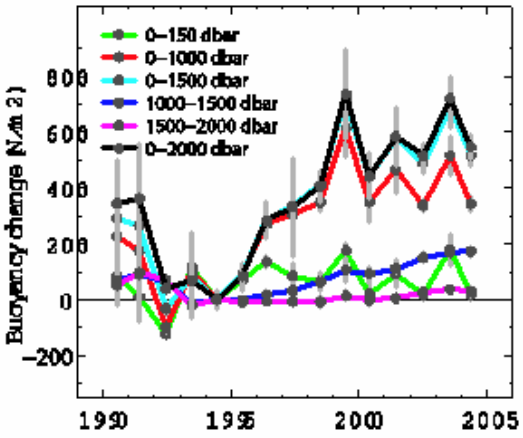

Fig. 10(c) Buoyancy content in selected layers relative to the 1994 value from spring and early summer AR7W occupations averaged over stations in the 320-520 km distance range as in Fig. 10(a).

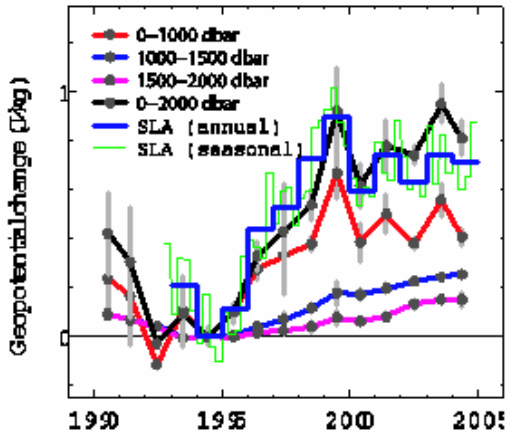

Fig. 10(d) Geopotential from hydrography for selected layers from spring and early summer AR7W occupations as in Fig. 10(a) and geopotential from altimetric sea level measurements relative to the 1994 mean as in Fig. 3(a).